

Diffusiophoresis in a Near-critical Binary Fluid Mixture

Youhei Fujitani*

School of Fundamental Science and Technology, Keio University, Yokohama 223-8522, Japan

(Dated: November 25, 2021)

We suppose that a rigid spherical particle is put into a binary fluid mixture with the critical composition in the homogeneous phase near the demixing critical point. A short-range interaction is assumed between each component and the particle surface, and one component is assumed to be attracted more than the other by the surface. The adsorption layer, where the preferred component is more concentrated, can be significantly thick owing to a large susceptibility. In this situation, an imposed composition gradient causes a particle motion, *i.e.*, diffusiophoresis emerges from a mechanism not considered previously. We calculate how the mobility depends on the temperature and particle size.

PACS numbers: 47.60.+i, 82.70.Dd, 47.55.dr

Diffusiophoresis and diffusioosmosis [1–6] have recently attracted much attention owing to their applications in lab-on-a-chip processes [7–14]. They are conventionally discussed in terms of a solution in contact with a solid. A solution in the interfacial layer, generated immediately near a solid surface, can have distinct properties due to some interaction potential between a solute and a surface. When a gradient of solute concentration is imposed in the direction tangential to the surface, some force exerted on only the solution in the interfacial layer can yield the slip velocity between the solid and the bulk of the solution. Diffusiophoresis occurs when a solution has no convection far from a mobile surface, whereas diffusioosmosis occurs when a surface is fixed. If the solution is electrolyte, the interfacial layer is the electric double layer. Otherwise, the layer can be generated by the van der Waals interaction or some dipole-dipole interaction.

Below, a binary fluid mixture, containing no ions, in the homogeneous phase close to the demixing critical point is considered and is simply referred to as a mixture. For flow having a typical length sufficiently large as compared with the correlation length of the composition fluctuation, we can apply hydrodynamics because the critical fluctuation occurs only on smaller length scales [15, 16]. Suppose that a rigid spherical particle is put into a mixture with the critical composition. A short-range interaction is assumed between each mixture component and the particle surface. One component is usually attracted more than the other by the surface [17–22], although it is not always the case [23, 24]. The adsorption layer, where the preferred component is more concentrated, can become significantly thick because of a large osmotic susceptibility. Assuming a mixture to be quiescent far from the particle, we previously calculated how the preferential adsorption (PA) affects the drag coefficient γ_d , which is defined as the negative of the ratio of the drag force to a given particle velocity in the linear regime [25].

We write T for the temperature, T_{cr} for the critical

temperature, and τ for $|T - T_{cr}|/T_{cr}$. In the renormalized local functional theory [26, 27], the free-energy functional (FEF) is coarse-grained up to the local correlation length, ξ . After coarse-grained, the equilibrium profile of the composition minimizes the FEF because many profiles different only on smaller length scales are unified into much fewer profiles [27, 28]. The hydrodynamics formulated from the coarse-grained FEF [29, 30] is used in our previous work [25]. Far from the particle, the composition is critical and ξ becomes equal to $\xi_0\tau^{-\nu}$, which is denoted by ξ_∞ . Here, ξ_0 is a non-universal length of molecular size, and ν (≈ 0.630) is a critical exponent [31]. The PA significantly affects γ_d if the particle radius, r_0 , is not much larger than ξ_∞ , which can indicate the thickness of the adsorption layer [25]. Near the particle, ξ can be much smaller than ξ_∞ in the presence of PA. Thus, even if r_0 is not much larger than ξ_∞ , ξ can be sufficiently small anywhere as compared with a typical length of the flow, in Ref. [25]. Experimentally, ξ_∞ can reach 100 nm.

In this Letter, we discuss diffusiophoresis due to the PA onto the particle surface by using the hydrodynamics mentioned above. As shown in Fig. 1, a particle lies in a mixture filled in a channel, which extends along the z axis and has the cross section and length much larger than r_0 . We impose a slight composition difference between the reservoirs to make a weak composition gradient in the channel. The particle undergoes a stationary and translational motion free from the drag force. In Fig. 1(b), we take a mixture region containing the particle. Far from the particle in this region, which is assumed to have a side length much larger than ξ_∞ , the composition gradient becomes a constant vector and convection vanishes. In the following paragraphs, we formulate this situation and calculate the mobility, which represents the ratio of the particle velocity to the constant vector. An anisotropic stress in the adsorption layer causes diffusiophoresis and originates from the free energy in the bulk of a mixture, which does not involve any potential due to the surface because the length range each component interacts with the surface is invisible in our coarse-grained description. This mechanism is not considered in the conventional theory. In our problem, a larger osmotic sus-

*Electronic address: youhei@appi.keio.ac.jp

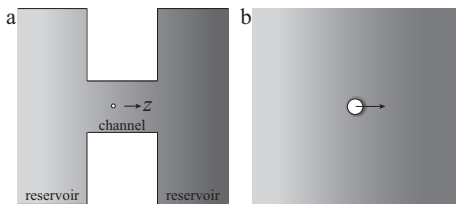


FIG. 1: Schematic of the situation supposed in our formulation. The gray scale indicates the composition; a component is more concentrated in a darker region. (a) A mixture is filled in a container, where a channel connects two reservoirs. A particle, represented by a circle, passes through the channel, which extends along the z axis. (b) A magnified view of a region including the particle. A darker region immediately near the particle represents the adsorption layer. The particle motion is represented by an arrow.

ceptibility should tend to increase the mobility in magnitude by thickening the adsorption layer, and have the opposite tendency by weakening the chemical-potential gradient under a given composition gradient. It is thus expected that the change of the mobility with τ can be nonmonotonic. The change with r_0 is expected to be explicit unless ξ_∞/r_0 is much smaller than unity. Our results are later shown to be consistent with these expectations. The dependence of the mobility on τ and r_0 may be utilized in manipulation of colloidal particles.

Referring to the mixture components as a and b, we write ρ_n for the mass density of the component n ($= a$ or b), and μ_n for the chemical potential conjugate to ρ_n . We write ρ for $\rho_a + \rho_b$, φ for $\rho_a - \rho_b$, and φ_c for the value of φ at the critical composition. Hereafter, a quantity at the critical composition is generally indicated by the subscript c . The order parameter is given by $\psi \equiv \varphi - \varphi_c$. The chemical potential conjugate to φ is given by $(\mu_a - \mu_b)/2$, and its deviation from the value at the critical point is denoted by μ . We write c_n for the mass fraction of the component n ; $c_n = \rho_n/\rho$ and $\varphi = \rho(2c_a - 1)$ hold. We can impose the composition gradient in the channel by making c_a different between the reservoirs. We use the conventional symbols for the critical exponents, β , γ , and η . The exponent η is approximately 0.0364 [31]; the (hyper)scaling relations give $2\beta + \gamma = 3\nu$ and $\gamma = \nu(2 - \eta)$.

The coarse-grained FEF is separated into the ρ -dependent part and ψ -dependent part. The latter part in the bulk of a mixture, $\mathcal{F}_b[\psi]$, is given by the volume integral of

$$f_b(\psi) + \frac{1}{2}K(\psi)|\nabla\psi|^2 - \mu\varphi \quad (1)$$

over the mixture. The functions $f_b(\psi)$ and $K(\psi)$ are derived in Ref. [27]; f_b is an even function and K is a positive function [32]. The corresponding integrand for the ρ -dependent part is independent of the derivatives of ρ . Difference in the interaction with the surface between the components contributes to the FEF and is described by the area integration of a function of φ over the particle

surface. Assuming it to be a linear function, we write h for the negative of the coefficient of φ ; h is called the surface field. The sum of the area integration and $\mathcal{F}_b[\psi]$ gives the ψ -dependent part, denoted by $\mathcal{F}[\psi]$. At the equilibrium, μ is homogeneous. In general, μ can depend on the position \mathbf{r} , ψ minimizing $\mathcal{F}[\psi]$ gives the coarse-grained profile, and the minimum of $\mathcal{F}[\psi]$ gives a part of the grand potential.

The reversible part of the pressure tensor originating from \mathcal{F}_b is denoted by Π . We can define p so that $p\mathbf{1}$ is the one from the ρ -dependent part. Here, $\mathbf{1}$ denotes the second-order isotropic tensor whose components are represented by Kronecker's delta, and p is the scalar pressure in the absence of \mathcal{F} . The reversible part of the pressure tensor is thus given by $p\mathbf{1} + \Pi$ in the bulk of a mixture. As in the model H [33], Π is obtained by subtracting the product of $\mathbf{1}$ and Eq. (1) from $K\nabla\psi\nabla\psi$ [34, 35]. If ψ is homogeneous, the scalar pressure, denoted by P , equals $p - f_b(\psi) + \mu\varphi$.

In the reference state, which is defined as the state a particle at rest lies in an equilibrium mixture with the critical composition far from the particle, μ vanishes and ρ is homogeneous. On this state, a composition gradient is imposed as a perturbation. Assuming that the gradient contains a smallness parameter ε , we calculate the velocity of a force-free particle up to the order of ε . In a frame fixed to the container, we define U so that the particle velocity equals $\varepsilon U\mathbf{e}_z$ up to the order of ε , where \mathbf{e}_z is the unit vector along the z axis. Far from the particle in Fig. 1(b), because no pressure gradient is imposed and no PA is assumed onto the channel wall, ∇P vanishes and the interdiffusion between the components occurs without convection [36]. There, the composition gradient is proportional to $\nabla\mu$ multiplied by the osmotic susceptibility. In the following calculation up to the order of ε , we first assume $\nabla\mu$ to be given far from the particle.

In the perturbed state, the time derivative of ρ vanishes in the frame co-moving with the particle center, and the velocity field \mathbf{v} satisfies the incompressibility condition $\nabla \cdot \mathbf{v} = 0$ up to the order of ε . The time derivative of φ is equal to the negative of the divergence of the sum of the convective flux, $\varphi\mathbf{v}$, and the diffusive flux. The latter is given by $-L(\psi)\nabla\mu$, where a function $L(\psi)$ represents the transport coefficient for the interdiffusion. We thus have $(\mathbf{v} - \varepsilon U\mathbf{e}_z) \cdot \nabla\psi = \nabla \cdot [L(\psi)\nabla\mu]$ with the aid of the stationarity in the co-moving frame and the incompressibility condition. We consider a particular instant, when the particle center passes the origin of the polar coordinate system (r, θ, ϕ) fixed to the container. The z axis is taken as the polar axis. A mixture does not diffuse into the particle, which yields $\partial_r\mu = 0$ at $r = r_0$. Here, ∂_r indicates the partial derivative with respect to r .

The convection of the correlated clusters of the order parameter, occurring on length scales smaller than ξ , enhances L [37, 38]. The diffusion coefficient describing the relaxation of the order-parameter fluctuation about the equilibrium in a mixture with the critical composition is given by the quotient of $L(0)$ divided by the

osmotic susceptibility. According to the mode-coupling theory [34, 37], the quotient is found to be the self-diffusion coefficient obtained by applying the Stokes law [39] and Sutherland-Einstein relation [40, 41] for a rigid sphere having a radius equal to ξ . We extend this result straightforwardly to a homogeneous off-critical composition, and apply the extended result in the dynamics, as in Ref. [25]. Thus, writing k_B for the Boltzmann constant, we use $L(\psi) = k_B T / [6\pi\eta_s \xi f_b''(\psi)]$, where ξ and ψ are regarded as their respective local values. The prime indicates the derivative with respect to the variable, and the double prime the second-order derivative. The osmotic susceptibility, with T and ρ being kept constant, is given by $1/f_b''(\psi)$, which is proportional to $\tau^{-\gamma}$ for $\psi = 0$ in the critical regime. As in the mode-coupling theory, we assume the shear viscosity, η_s , to be a constant, neglecting its weak singularity. With the aid of $\nabla \cdot \Pi = \varphi \nabla \mu$, we use the Stokes approximation to have $0 = -\nabla p - \varphi \nabla \mu + \eta_s \Delta \mathbf{v}$, which represents the momentum conservation. By assuming the no-slip boundary condition, we have $\mathbf{v} = \varepsilon U \mathbf{e}_z$ at $r = r_0$.

A superscript (0) is added to a field in the reference state. For ψ in this state, we can write $\psi^{(0)}(r)$ because of the symmetry. We define p_+ as $p + \varphi_c \mu$. Up to the order of ε , we expand the fields as $p_+(\mathbf{r}) = p_+^{(0)}(r) + \varepsilon p_+^{(1)}(\mathbf{r})$, $\mu(\mathbf{r}) = \varepsilon \mu^{(1)}(\mathbf{r})$, and $\mathbf{v}(\mathbf{r}) = \varepsilon \mathbf{v}^{(1)}(\mathbf{r})$. A field with the superscript (1) is defined so that it becomes at the order of ε after multiplied by ε . Far from the particle, $p_+^{(1)}$ becomes constant because there $\varepsilon p_+^{(1)}$ equals P at the order of ε . Up to the order of ε , the interdiffusion is described by

$$\left(\mathbf{v}^{(1)} - U \mathbf{e}_z \right) \cdot \nabla \psi^{(0)} = \nabla \cdot \left[L(\psi^{(0)}) \nabla \mu^{(1)} \right], \quad (2)$$

and the momentum conservation by

$$0 = -\nabla p_+^{(1)} - \psi^{(0)} \nabla \mu^{(1)} + \eta_s \Delta \mathbf{v}^{(1)}. \quad (3)$$

We define τ_* as $(\xi_0/r_0)^{1/\nu}$ to use $\hat{\tau} \equiv \tau/\tau_*$, and define L_* as $L(0)$ at $\tau = \tau_*$ to have $L(0) = \hat{\tau}^{\nu\eta-\nu} L_*$. Because of the particle-motion symmetry, the angular dependence of $\mu^{(1)}$ and that of $v_r^{(1)}$ are only via $\cos \theta$, that of $v_\theta^{(1)}(\mathbf{r})$ only via $\sin \theta$, and $v_\phi^{(1)}$ vanishes [42]. Writing \hat{r} for r/r_0 , we define dimensionless functions, \mathcal{Q} and \mathcal{R} , so that

$$\mathcal{Q}(\hat{r}) \cos \theta = \frac{\sqrt{L_*} \mu^{(1)}(\mathbf{r})}{U \sqrt{5\eta_s}} \quad \text{and} \quad \mathcal{R}(\hat{r}) \cos \theta = \frac{v_r^{(1)}(\mathbf{r})}{U} \quad (4)$$

hold [43]. We rewrite Eq. (2) as

$$\mathcal{D}_{-1} \mathcal{D}_2 \mathcal{Q}(\hat{r}) = -3\Phi(\hat{r}) [\mathcal{A}(\hat{r}) (\mathcal{R}(\hat{r}) - 1) - \mathcal{B}(\hat{r}) \mathcal{Q}'(\hat{r})], \quad (5)$$

where \mathcal{D}_m represents $\hat{r} \partial_{\hat{r}} + m$ and $\Phi(\hat{r})$ is defined as $-r^2 \psi^{(0)'}(r_0 \hat{r}) / [3\sqrt{5\eta_s} L_*]$. Definitions of the functions \mathcal{A} and \mathcal{B} are shown in Supplemental Material [32]. From Eq. (3), we eliminate $p_+^{(1)}$ to obtain

$$\mathcal{D}_1 \mathcal{D}_{-2} \mathcal{D}_3 \mathcal{D}_0 \mathcal{R}(\hat{r}) = -30\Phi(\hat{r}) \mathcal{Q}(\hat{r}). \quad (6)$$

These two equations are derived in Ref. [25]. The boundary conditions for \mathcal{Q} and \mathcal{R} , respectively derived from those for \mathbf{v} and μ , are the same as given in Ref. [25] except that $\mathcal{Q}(\hat{r})$ is proportional to \hat{r} far from the particle [32]. We write g for the constant of proportionality; Ref. [25] supposes $g = 0$.

Taking the boundary conditions into account, we can transform Eq. (5) into the form that \mathcal{Q} equals the sum of the solution in the absence of the right-hand side (RHS) and the convolution of a kernel and the RHS. Equation (6) can be transformed similarly by using another kernel. The kernels, after multiplied by numerical factors, are respectively denoted by Γ_Q and Γ_R , which are given in Appendix of Ref. [25]. As in this reference, we assume that the RHSs are multiplied by an artificial parameter κ . Accordingly, we rewrite \mathcal{Q} as $\tilde{\mathcal{Q}}_\kappa$ and \mathcal{R} as $\tilde{\mathcal{R}}_\kappa$. We find $\tilde{\mathcal{Q}}_0(\hat{r})$ equal to $g(\hat{r} + (\hat{r}^{-2}/2))$, which is below referred to as $q_0(\hat{r})$ [32]. Eliminating $\tilde{\mathcal{R}}_\kappa$ from the two integral equations, and expanding $\tilde{\mathcal{Q}}_\kappa$ with respect to κ as $\tilde{\mathcal{Q}}_\kappa(\hat{r}) = \sum_{n=0}^{\infty} q_n(\hat{r}) \kappa^n$, we obtain a recurrence relation for the expansion coefficients, denoted by q_n , as

$$q_n(\hat{r}) = \int_1^\infty d\hat{s} \Gamma_Q(\hat{r}, \hat{s}) \Phi(\hat{s}) \left[-\mathcal{B}(\hat{s}) q'_{n-1}(\hat{s}) + \mathcal{A}(\hat{s}) \int_1^\infty d\hat{u} \Gamma_R(\hat{s}, \hat{u}) \Phi(\hat{u}) q_{n-2}(\hat{u}) \right] \quad (7)$$

for $n = 1, 2, 3, \dots$. Here, for $n = 1$, the integral with respect to \hat{u} is replaced by $\alpha_0(\hat{s}) \equiv (3\hat{s}^{-1}/2) - (\hat{s}^{-3}/2) - 1$. The original solutions of \mathcal{Q} and \mathcal{R} are respectively given by $\tilde{\mathcal{Q}}_1$ and $\tilde{\mathcal{R}}_1$.

The drag coefficient for a value of g in general deviates from the Stokes law, $6\pi\eta_s r_0$, owing to the PA and the imposed gradient. Equation (3.28) of Ref. [25] is still valid for the drag coefficient considered here. Thus, writing $\Delta\hat{\gamma}_d$ for the ratio of the deviation to the Stokes law, we find $\Delta\hat{\gamma}_d$ to be given by the integral of $10\alpha_0(\hat{r})\Phi(\hat{r})\mathcal{Q}(\hat{r})/3$ from $\hat{r} = 1$ to ∞ . Obtaining q_n from Eq. (7) and replacing \mathcal{Q} by q_n in the integral above, we find that the sum of the integrals over $n = 0, 1, 2, \dots$ gives $\Delta\hat{\gamma}_d$. We truncate this series suitably to calculate $\Delta\hat{\gamma}_d$ numerically [44]. From the governing equations and the boundary conditions for \mathcal{Q} and \mathcal{R} , we find $\Delta\hat{\gamma}_d$ to be a linear function of g . The linear function, which is obtained by calculating $\Delta\hat{\gamma}_d$ for $g = 0$ and 1, determines the value of g making the drag force vanish. This value is denoted by g_0 . From the fact that the sign of $\psi^{(0)}(r)$ is changed by changing that of h , we find g_0 to be an odd function of h [32].

When $\nabla \mu$ ($\propto \mathbf{e}_z$) is given far from the particle, the velocity of a force-free particle equals the product of $(r_0 \sqrt{L_*}/5\eta_s/g_0)$ and the given gradient, because of the first entry of Eq. (4). Below, we use the parameter values [32] by supposing a mixture of 2,6-lutidine and water (LW), which has $T_{cr} = 307$ K, $c_{ac} = 0.290$, and $\xi_0 = 0.198$ nm [45]. In Fig. 2(a), we find for $h > 0$ that $1/g_0$, being positive, increases as τ decreases and as h increases. This increase of $1/g_0$ is expected because

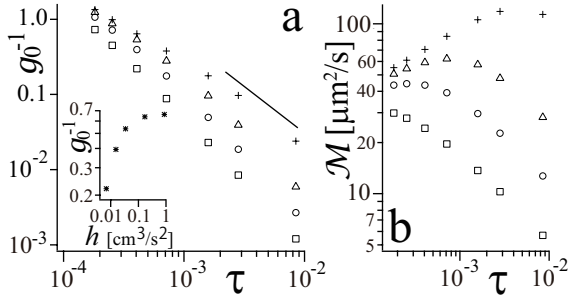


FIG. 2: Plots of $1/g_0$ (a) and \mathcal{M} (b) against τ for $r_0 = 0.1 \mu\text{m}$. The results shown by the symbols $+$, \triangle , \circ , and \square are respectively obtained for $h = 1.73 \times 10^{-1}$, 3.46×10^{-2} , 1.55×10^{-2} , and $6.91 \times 10^{-3} \text{ cm}^3/\text{s}^2$. The reference line in (a) has the slope of $-\gamma$. In the inset, $1/g_0$ is plotted against h for $\tau = 4.05 \times 10^{-4}$ and $r_0 = 0.1 \mu\text{m}$.

then, as shown in Ref. [32], the PA is stronger. In the inset of Fig. 2(a), the increase of $1/g_0$ with h becomes more gradual as h increases for the value of τ . In Supplemental Material [32], flows around a force-free particle are examined for some parameter values, and they are shown to be consistent with our coarse-grained description.

To consider the diffusiophoretic mobility, we assume that ∇c_a ($\propto e_z$) is given far from the particle. Writing $c'_{a\infty}$ for the z component of the given gradient, we define the mobility \mathcal{M} so that $\varepsilon U = \mathcal{M} c'_{a\infty}/c_{ac}$ holds, and have

$$\mathcal{M} = \frac{r_0 c_{ac} \sqrt{L_*}}{g_0 \sqrt{5} \eta_s} \times \left. \frac{\partial \mu}{\partial c_a} \right|_{TP}. \quad (8)$$

Here, the partial derivative, with (T, P) fixed, is evaluated far from the particle in the reference state. It is positive because of the thermodynamic stability. Thus, the particle moves towards the reservoir where the component preferred by the particle surface is more concentrated, as shown in Fig. 1(b). The conventional diffusiophoresis has a similar property [5, 6]. In our formulation, the partial derivative approximately equals $2\rho_c f_b''(0)$ ($\propto \tau^\gamma$) [32], and thus \mathcal{M} can be calculated. In Fig. 2(b), the slope of \mathcal{M} is negative at $\tau \approx 10^{-2}$ for each value of h . Except for the smallest value of h , the slope is positive for small τ and the value of τ at the peak of \mathcal{M} increases with h . This is expected from Fig. 2(a), because the slope should become negative when the decrease of $1/g_0$ with increasing τ overcomes the increase of τ^γ . In Fig. 3, \mathcal{M} increases with r_0 , as in the conventional theory [5, 47]. The increase is explicit in particular when r_0 is smaller than approximately $0.2 \mu\text{m}$ at the larger value of τ .

Suppose that the difference in c_a between the reservoirs is $c_{ac}/10$ and that the channel length is $10 \mu\text{m}$. The composition then stays near the critical one over the channel. If we adopt $\mathcal{M} = 50 \mu\text{m}^2/\text{s}$ from Fig. 2(b), the particle speed is $0.5 \mu\text{m}/\text{s}$ for $r_0 = 0.1 \mu\text{m}$. For $\psi^{(0)}$ to be distinguished from the fields at the order of ε in Eqs. (2) and (3), the influence of the imposed composition gradi-

ent is required to be negligible in the adsorption layer. This requirement is fulfilled in the example considered here, as shown in Supplemental Material [32]. As τ increases well beyond the range of Fig. 2, ξ_∞ approaches a molecular size and the anisotropic stress becomes ill-defined. Then, because of the background contribution to the osmotic susceptibility [38, 46], the partial derivative in Eq. (8) should stop increasing in proportion to τ^γ . The mobility should be then explained not by the PA but by the conventional mechanism.

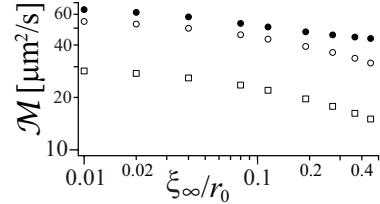


FIG. 3: Plots of \mathcal{M} against ξ_∞/r_0 . Solid and open circles represent the results for $\tau = 1.82 \times 10^{-4}$ and 7.14×10^{-4} , respectively, under $h = 1.55 \times 10^{-2} \text{ cm}^3/\text{s}^2$. For these values of τ , ξ_∞ equals 45.0 and 19.0 nm, respectively. Squares represent the results for $\tau = 7.14 \times 10^{-4}$ and $h = 6.91 \times 10^{-3} \text{ cm}^3/\text{s}^2$.

It is shown in Ref. [47] that, for nanocolloids in a nonelectrolyte solution, the diffusiophoretic mobility in the conventional theory can be also obtained by the molecular dynamics simulation. We naively convert the second result from the right end in their Fig. 3(c) to $\mathcal{M} = 1.6 \times 10^2 \mu\text{m}^2/\text{s}$ for a mixture of LW by taking 2,6-lutidine as the component a and by using $k_B T_{\text{cr}}$ and ξ_0 as the unit energy and length, respectively. The potential for the interaction between the nanocolloid and the solute is mentioned in Ref. [47]. Regarding it as representing the adsorption of the component a and assuming the length range of the interaction to have the unit length, we tentatively convert its value at the surface of the immobile region to $h = 1.0 \text{ cm}^3/\text{s}^2$. Thus, neglecting the dependence of the converted mobility on r_0 , we can deduce that the values of \mathcal{M} shown by the cross and square in Fig. 2(b) of the present study would approximately become 60 and $10 \mu\text{m}^2/\text{s}$, respectively, in the range of τ validating the conventional theory. It is thus possible, for $h > 0$, that the mobility for large h is made smaller inside the critical regime than outside by larger osmotic susceptibility, and that the mobility for small h is made larger by thicker adsorption layer. This possibility clearly needs further investigation, in particular because the converted values depend considerably on the unit length.

In this Letter, for diffusiophoresis in a nonelectrolyte fluid mixture near the demixing critical point, we theoretically show that the mobility can have a magnitude large enough to be detected, that its dependence on the temperature can be changed qualitatively by the surface field, and that its dependence on the particle radius can remain explicit even if the radius exceeds $0.1 \mu\text{m}$.

The author thanks Dr. S. Yabunaka for stimulating discussions.

Supplemental Material

In Ref. [27], the coarse-grained FEF is derived from the Ginzburg-Landau-Wilson type of bare model and contains ξ_0 , C_1 and C_2 as material constants. They are linked by $C_2 = 3u^*C_1\xi_0$, where u^* denotes the scaled coupling constant at the Wilson-Fisher fixed point and equals $2\pi^2/9$ in the three dimensions at the one loop order. The “distance” from the critical point is represented by $\omega \equiv (\xi_0/\xi)^{1/\nu}$. We have $\omega = \tau$ if ψ vanishes, and write $\hat{\omega}$ for ω/τ_* . A dimensionless order parameter is defined as $\hat{\psi}(\hat{r}) \equiv \psi(r_0\hat{r})/\psi_*$, where ψ_* denotes $\tau_*^\beta/\sqrt{C_2}$. Introducing $\mu_* \equiv k_B T/(3u^*r_0^3\psi_*)$, we use dimensionless quantities, $\hat{\mu} \equiv \mu/\mu_*$ and $\hat{h} \equiv h/(\mu_*r_0)$. The function $K(\psi)$ equals $k_B T C_1 \omega^{-n\nu}$, whereas $f_b(\psi)$ equals $\mu_*\psi_*\hat{f}_b(\psi/\psi_*)$ with a dimensionless function \hat{f}_b being defined as

$$\hat{f}_b(\hat{\psi}) = \hat{\omega}^{\gamma-1}\hat{\tau} \left(\frac{\hat{\psi}^2}{2} + \frac{\hat{\psi}^4}{12\hat{\omega}^{2\beta-1}\hat{\tau}} \right). \quad (9)$$

Here and in the following, $\hat{\omega}$ is regarded as a function of $\hat{\psi}$ because we have a self-consistent condition, $\hat{\omega} = \hat{\tau} + \hat{\omega}^{1-2\beta}\hat{\psi}^2$.

The equilibrium profile $\psi^{(0)}$, vanishing far from the particle, equals ψ minimizing $\mathcal{F}[\psi]$ under $\mu = 0$. The stationary condition yields

$$\hat{f}'_b = -\frac{\eta\nu}{2} \frac{\hat{\omega}'}{\hat{\omega}^{\eta\nu+1}} \left(\partial_{\hat{r}}\hat{\psi} \right)^2 + \frac{1}{\hat{\omega}^{\eta\nu}} \left(\partial_{\hat{r}}^2 + \frac{2}{\hat{r}}\partial_{\hat{r}} \right) \hat{\psi} \quad (10)$$

for $\hat{r} > 1$, together with $\partial_{\hat{r}}\hat{\psi} = -\hat{h}\hat{\omega}^{\eta\nu}$ at $\hat{r} = 1$. Thus, $\hat{\psi}^{(0)}$ is totally determined by $\hat{\tau}$ and \hat{h} . We can rewrite Φ as $\Phi(\hat{r}) = -\hat{r}^2\partial_{\hat{r}}\hat{\psi}^{(0)}(\hat{r})/\sqrt{5\pi}$. The functions of \mathcal{A} and \mathcal{B} are defined as $\mathcal{A}(\hat{r}) \equiv L_*/L(\psi^{(0)}(r_0\hat{r})) = \hat{f}''_b/\hat{\omega}^\nu$ and

$$\mathcal{B}(\hat{r}) \equiv \sqrt{5\eta_s L_*} \frac{L'(\psi^{(0)}(r_0\hat{r}))}{r_0 L(\psi^{(0)}(r_0\hat{r}))} = \sqrt{\frac{5\pi}{9}} \left(\nu \frac{\hat{\omega}'}{\hat{\omega}} - \frac{\hat{f}'''_b}{\hat{f}''_b} \right). \quad (11)$$

Thus, \mathcal{Q} and \mathcal{R} are totally determined by g , $\hat{\tau}$ and \hat{h} , which means that g_0 is totally determined by $\hat{\tau}$ and \hat{h} . If the sign of h is changed, the signs of Φ and \mathcal{B} are changed, whereas \mathcal{A} is unchanged. Then, if that of g is also changed, that of \mathcal{Q} is changed, whereas \mathcal{R} and $\Delta\hat{\gamma}_d$ are unchanged. Thus, g_0 is an odd function of h .

A mixture of LW is supposed below. In Ref. [48], $C_2 = 7.14 \times 10^{-7} \text{ m}^6/\text{kg}^2$ is obtained from the experimental data [45, 49, 50] with the aid of Eqs. (3.3) and (3.23) of Ref. [27]. This value yields $\psi_* = 4.70 \times 10 \text{ kg}/\text{m}^3$ for $r_0 = 0.1 \text{ }\mu\text{m}$. In particular when 2,6-lutidine preferentially adsorbs onto the particle surface, it gives a good approximation to regard η_s as a constant in the range of τ examined, thanks to the background contribution [48]. In practice, this adsorption occurs for a silica particle [51]. We use $\eta_s = 2.43 \text{ mPa}\cdot\text{s}$ from the data in Refs. [52, 53].

We obtain $\hat{\psi}^{(0)}$ by numerically solving Eq. (10) and the boundary conditions mentioned around this equation. In

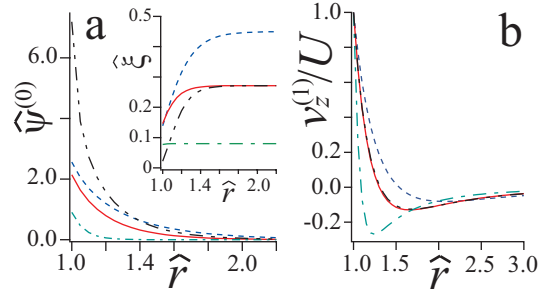


FIG. 4: Against \hat{r} , $\hat{\psi}^{(0)}(\hat{r})$ is plotted in (a), $\hat{\xi}$ in the reference state is plotted in the inset, and $v_z^{(1)}/U$ at $\theta = \pi/2$ in (b) for $r_0 = 0.1 \text{ }\mu\text{m}$. The blue dashed, red solid, and green dash-dot curves are obtained for $\tau = 1.82 \times 10^{-4}$, 4.05×10^{-4} , and 2.82×10^{-3} , respectively, under $h = 1.55 \times 10^{-2} \text{ cm}^3/\text{s}^2$. The black dash-dot-dot curve is obtained for $\tau = 4.05 \times 10^{-4}$ and $h = 1.73 \times 10^{-1} \text{ cm}^3/\text{s}^2$.

Fig. 4(a), $\hat{\psi}^{(0)}$ decreases as \hat{r} increases. The decrease is more gradual as τ decreases, which implies that the adsorption layer then becomes thicker. The value of $\hat{\psi}^{(0)}(1)$ is larger as h increases. We define $\hat{\xi}$ as $\xi/r_0 \equiv \hat{\omega}^{-\nu}$, calculate its values in the reference state with the aid of the self-consistent condition, and plot the results in the inset of Fig. 4(a). The value of $\hat{\xi}$ near the particle surface is smaller than $\xi_\infty/r_0 = \hat{\tau}^{-\nu}$, because there the composition deviates from the critical one.

We obtain $v_\theta^{(1)}/U = -\sin\theta[\partial_{\hat{r}}\hat{r}^2\mathcal{R}(\hat{r})]/(2\hat{r})$ with the aid of the incompressibility condition. The boundary conditions for \mathcal{Q} and \mathcal{R} at $\hat{r} = 1$ are $\mathcal{Q}' = 0$, $\mathcal{R} = 1$, and $\mathcal{R}' = 0$. Far from the particle, \mathcal{R} vanishes and $\mathcal{Q}(\hat{r})$ becomes $g\hat{r}$. We note that g_0 satisfies the boundary conditions for \mathcal{Q} and deletes the left-hand side (LHS) of Eq. (6) of the main text. The differences of the solutions \mathcal{R} and \mathcal{Q} for $g = 0$ subtracted from the respective solutions for a value of g are found to be proportional to g , which means that $\Delta\hat{\gamma}_d$ is a linear function of g . For the force-free particle motion, *i.e.*, for $g = g_0$, we calculate \mathcal{R} and plot $v_z^{(1)}/U$ at $\theta = \pi/2$, *i.e.*, $\mathcal{R} + \hat{r}\partial_{\hat{r}}\mathcal{R}/2$, in Fig. 4(b). The value of unity at $\hat{r} = 1$ represents the no-slip boundary condition. For each set of (τ, h) , the sign of the plotted function changes from positive to negative as \hat{r} increases. Its zero is larger as τ decreases for $h = 1.55 \times 10^{-2} \text{ cm}^3/\text{s}^2$. The curves for $\tau = 4.05 \times 10^{-4}$ and the different values of h approximately coincide with each other. Although data not shown, this approximate coincidence is also observed for each of the other values of τ . These properties are reasonable, considering that ξ_∞ indicates the thickness of the adsorption layer. Notably, each curve in Fig. 4(b) can be traced approximately if it is viewed with the local resolution given by the corresponding local value of $\hat{\xi}$ shown in the inset of Fig. 4(a). This is required in our coarse-grained description.

We write \bar{v}_n for the partial volume par unit mass of the component n , and write \bar{v}_\pm for $(\bar{v}_a \pm \bar{v}_b)/2$. If the

mass densities are homogeneous, we have

$$\left(\frac{\partial\mu}{\partial\varphi}\right)_{T\rho} = \left(\frac{\partial\mu}{\partial P}\right)_{Tc_a} \left(\frac{\partial P}{\partial\varphi}\right)_{T\rho} + \left(\frac{\partial\mu}{\partial c_a}\right)_{TP} \left(\frac{\partial c_a}{\partial\varphi}\right)_{T\rho}. \quad (12)$$

The LHS above equals $f_b''(\psi)$, whereas the first and second derivatives of the first term on the RHS equal \bar{v}_- and $f_b''(\psi)\varphi$, respectively. Thus, with the aid of the identity $1 = \bar{v}_a\rho_a + \bar{v}_b\rho_b$, we obtain

$$\left(\frac{\partial\mu}{\partial c_a}\right)_{TP} = 2\rho_c^2\bar{v}_{+c}f_b''(0) \quad (13)$$

far from the particle in the reference state. This can be substituted into Eq. (8) of the main text. From the data in Table III of Ref. [49], we estimate $\bar{v}_a = 1.03 \times 10^{-3} \text{ m}^3/\text{kg}$ and $\bar{v}_b = 1.00 \times 10^{-3} \text{ m}^3/\text{kg}$ for a mixture of LW lying in the homogeneous phase near the demixing critical point [48]. Thus, the mixture has $\bar{v}_{+c} \approx 1/\rho_c$. In our formulation, because of $f_b''(0) = k_B T C_1 \tau^\gamma / \xi_0^2$, we have $L_* = (\xi_0/r_0)^\gamma r_0 / (6\pi\eta_s C_1)$.

An example with $c'_{a\infty}/c_{ac} = 0.01 \mu\text{m}^{-1}$ and $r_0 = 0.1 \mu\text{m}$ is discussed in the main text. Using these val-

ues, we find $2r_0\partial_z\hat{\psi}$ far from the particle to be 2×10^{-2} approximately. To this value, the ratio of the change of $\hat{\psi}$ from $\theta = 0$ to π immediately near the particle is equal to \mathcal{Q}/f_b'' at $\hat{r} = 1$ divided by $g_0/f_b''(0)$, up to the order of ε . The ratios $\mathcal{Q}(1)/g_0$ and $H \equiv f_b''(0)/f_b''(\psi^{(0)}(r_0))$, together with $\hat{\psi}^{(0)}(1)$, are shown for some sets of (τ, h) in Table I [54]. The change is found to be much smaller than $\hat{\psi}^{(0)}(1)$ in the example, as required for the validity of our perturbation calculation. If r_0 is larger, the imposed composition gradient may be required to be smaller in magnitude, depending on the values of τ and h .

TABLE I: Values of $(\mathcal{Q}(1)/g_0, H, \hat{\psi}^{(0)}(1))$ for $r_0 = 0.1 \mu\text{m}$.

$h [\text{cm}^3/\text{s}^2]$	$\tau = 1.82 \times 10^{-4}$	$\tau = 2.82 \times 10^{-3}$
6.91×10^{-3}	(1.4, 0.22, 1.5)	(1.5, 0.97, 0.41)
1.55×10^{-2}	(1.2, 0.048, 2.6)	(1.5, 0.87, 0.91)
1.73×10^{-1}	(0.63, 0.0011, 7.3)	(1.4, 0.047, 6.3)

-
- [1] B. V. Derjaguin, S. S. Dukhin, and V. V. Koptelova, *J. Coll. Interf. Sci.* **38**, 584 (1972).
- [2] J. L. Anderson, M. E. Lowell, and D. C. Prieve, *J. Fluid Mech.* **117**, 107 (1982).
- [3] J. L. Anderson and D. C. Prieve, *Sep. Purif. Methods* **13**, 67 (1984).
- [4] D. C. Prieve and R. Roman, *J. Chem. Soc., Faraday Trans. 2*, **83**, 1287 (1987).
- [5] J. L. Anderson, *Ann. Rev. Fluid Mech.* **21**, 61 (1989).
- [6] P. O. Staffeld and J. A. Quinn, *J. Coll. Interf. Sci.* **130**, 88 (1989).
- [7] B. Abécassis, C. Cottin-Bizonne, C. Ybert, A. Adjari and L. Bocquet, *New J. Phys.* **11**, 075022 (2009).
- [8] C. Lee, C. Cottin-Bizonne, A.-L. Biance, P. Jpseph, L. Bocquet, and C. Ybert, *Phys. Rev. Lett.* **112**, 244501 (2014).
- [9] A. Kar, T.-Y. Chang, I. O. Riviera, A. Sen, and D. Velegol, *ACS Nano* **9**, 746 (2015).
- [10] S. Shin, E. Urn, B. Sabass, J. T. Auit, M. Rahimi, P. B. Warren, and H. A. Stone, *Proc. Natl. Acad. Sci. USA* **113**, 257 (2016).
- [11] H. J. Keh, *Curr. Opin. Coll. Interf. Sci.* **24**, 13 (2016).
- [12] D. Velegol, A. Garg, R. Gusha, A. Kar, and M. Kumar, *Soft Matter* **12**, 4686 (2016).
- [13] S. Marbach and L. Bocquet, *Chem. Soc. Rev.* **48**, 3102 (2019).
- [14] S. Shin, *Phys. Fluids* **32**, 101302 (2020).
- [15] R. Okamoto, Y. Fujitani, and S. Komura, *J. Phys. Soc. Jpn* **82**, 084003 (2013).
- [16] A. Furukawa, A. Gambassi, S. Dietrich, and H. Tanaka, *Phys. Rev. Lett.* **111**, 055701 (2013).
- [17] J. W. Cahn, *J. Chem. Phys.* **66**, 3667 (1977).
- [18] D. Beysens and S. Leibler, *J. Physique Lett.* **43**, 133 (1982).
- [19] M. N. Binder, in *Phase Transitions and Critical Phenom-ena VIII*, edited by C. Domb and J. Lebowitz, (Academic, London, 1983).
- [20] D. Beysens, and D. Estève, *Phys. Rev. Lett.* **54**, 2123 (1985).
- [21] R. Holyst and A. Poniewierski, *Phys. Rev. B* **36**, 5628 (1987).
- [22] H. W. Diehl, *Int. J. Mod. Phys. B* **11**, 3503 (1997).
- [23] D. Beysens, *Thermodyn. Interf. Fluid Mech.* **3**, 1 (2019).
- [24] Y. Fujitani, *J. Fluid Mech.* **907**, A21 (2021).
- [25] S. Yabunaka and Y. Fujitani, *J. Fluid Mech.* **886** A2 (2020).
- [26] M. E. Fisher, and H. Au-Yang, *Physica A* **101**, 255 (1980).
- [27] R. Okamoto and A. Onuki, *J. Chem. Phys.* **136**, 114704 (2012).
- [28] S. Yabunaka and A. Onuki, *Phys. Rev. E* **96**, 032127 (2017).
- [29] S. Yabunaka, R. Okamoto, and A. Onuki, *Soft Matter* **11**, 5738 (2015).
- [30] Y. Fujitani, *J. Phys. Soc. Jpn.* **86**, 044602 (2017).
- [31] A. Pelissetto and E. Vicari, *Phys. Rep.* **368**, 549 (2002).
- [32] See Supplemental Material for additional figures and details, including the definitions of f_b and K and the parameter values other than shown in the text.
- [33] P. C. Hohenberg and B. I. Halperin, *Rev. Mod. Phys.* **49**, 435 (1977).
- [34] A. Onuki, *Phase Transition Dynamics* (Cambridge University Press, Cambridge, 2002), Chap. 6.1.
- [35] A. Onuki, *Phys. Rev. E* **55**, 403 (1997).
- [36] The PA onto the channel wall generates diffusioosmosis to convect a mixture in the channel in the presence of only the composition difference between the reservoirs, as shown in Ref. [48].
- [37] K. Kawasaki, *Ann. Phys. (N. Y.)* **61**, 1 (1970).
- [38] J. V. Sengers, *Int. J. Thermophys.* **6**, 203 (1985).

- [39] G. G. Stokes, *Trans. Camb. Phil. Soc.* **9**, 8 (1851).
- [40] W. Sutherland, *Phil. Mag.* **9**, 781 (1905).
- [41] A. Einstein, *Ann. Phys. (Leipzig)* **322**, 549 (1905).
- [42] Y. Fujitani, *J. Phys. Soc. Jpn.* **76**, 064401 (2007).
- [43] A possible constant term included in $\mu^{(1)}$ does not affect our calculation and is neglected.
- [44] We use the software Mathematica (Wolfram Research). Only for the result on the extreme right in the inset of Fig. 2(a), the series for $\Delta\hat{\gamma}_d$ numerically diverges, and the Borel summation is applied instead of the suitable truncation.
- [45] S. Z. Mirzaev, R. Behrends, T. Heimbürg, J. Haller, and U. Kaatze, *J. Chem. Phys.* **124** 144517 (2006).
- [46] H. L. Swinney and D. L. Henry, *Phys. Rev. A* **8**, 2586 (1973).
- [47] N. Sharifi-Mood, J. Koplik, and C. Maldarelli, *Phys. Rev. Lett.* **111**, 184501 (2013).
- [48] S. Yabunaka and Y. Fujitani, <http://arxiv.org/abs/2105.00466>.
- [49] Y. Jayalakshmi, J. S. van Duijneveldt, and D. Beysens, *J. Chem. Phys.* **100**, 604 (1994).
- [50] K. To, *Phys. Rev. E* **63**, 026108 (2001).
- [51] R. A. Omari, C. A. Grabowski & A. Mukhopadhyay, *Phys. Rev. Lett.* **103**, 225705 (2009).
- [52] A. Stein, S. J. Davidson, J. C. Allegra, and G. F. Allen, *J. Chem. Phys.* **56** 6164 (1972).
- [53] C. A. Grattoni, R. A. Dawe, C. Y. Seah, and J. D. Gray, *Chem. Eng. Data*, **38**, 516 (1993).
- [54] For some sets of (τ, h) in Table I, $\mathcal{Q}(1)/g_0$ is close to $q_0(1)/g = 3/2$.